Polysulfide Ligands in Solid-State Antimony Compounds. Isolation and Structural Characterization of $Cs_2Sb_4S_8$ and $CsSbS_6$

Timothy J. McCarthy and Mercouri G. Kanatzidis*,†

Department of Chemistry and the Center for Fundamental Materials Research, Michigan State University, East Lansing, Michigan 48824

Received August 18, 1993®

$Cs_2Sb_4S_8$ and $CsSbS_6$ were synthesized by reacting Sb with a Cs_2S_x flux. An investigation of the Sb/Cs_2S_x system at 260 and 280 °C revealed the presence of two new ternary sulfides, $Cs_2Sb_4S_8$ **(I)** (67% yield) and $CsSbS_6$ **(II)** (69% yield), respectively. Red-orange $Cs_2Sb_4S_8$ crystallizes in the triclinic $P\bar{1}$ space group (No. 2) with $a = 6.743(1)$ Å, $b = 9.577(2)$ Å, $c = 6.397(1)$ Å, $\alpha = 91.63(1)°$, $\beta = 104.83(1)°$, $\gamma = 80.57(1)°$, $V = 392$ Å^3, $Z = 1$, and $d_{calc} = 4.27$g/cm^3; number of data with $F_o^2 > 3\sigma(F_o^2)$ 1889, number of variables 65, $2\theta_{max} = 60°$. The final $R/R_w = 3.2/4.9$. The structure of **I** consists of $[Sb_4S_6]$ units that are assembled into chains in the a direction. The chains are connected by S_2^{2-} bridging units to form layers that are parallel to the (011) crystallographic plane. The layers are connected by Sb–S interactions to form channels that are filled with 10-coordinate Cs^+ ions (Cs–S mean = 3.62(4) Å). Compound **II** crystallizes in the $P2_1/n$ space group (No. 14) with $a = 5.885(2)$ Å, $b = 14.413(2)$ Å, $c = 11.079(2)$ Å, $\beta = 101.69(2)°$, $V = 920$ Å^3, $Z = 4$, and $d_{calc} = 3.23$g/cm^3; number of data with $F_o^2 > 3\sigma(F_o^2)$ 1926, number of variables 74, $2\theta_{max} = 60°$. The final $R/R_w = 2.5/3.9$. The structure consists of four-membered Sb_2S_2 rings linked along the a axis via pentasulfide ligands to form one-dimensional chains that are separated by Cs^+ ions. The band gaps of the semiconducting **I** and **II** are 2.05 and 2.25 eV, respectively. Thermal analysis data for I and II are reported.

Introduction

During the past two decades, a variety of synthetic routes have been employed for exploratory synthesis of solid-state ternary antimony sulfide compounds. Direct combination of the binary sulfides A_2S/Sb_2S_3 (A = Na, K, Rb, Cs) and $(AE)S/Sb_2S_3$ (AE = Ca, Sr, Ba) at high temperature has been used to obtain $ASbS_2$ (A = Na, K, Cs, Rb),[1] $Ca_2Sb_2S_5$,[2] $Ba_8Sb_6S_{17}$,[3] and $Sr_3Sb_4S_9$.[4] In addition, hydro(solvento)thermal reactions have yielded several additional phases, including $[N(C_3H_7)_4]Sb_3S_5$,[5] $(N_2C_4H_8)Sb_4S_7$,[5] $Cs_3Sb_5S_9$,[6] α,β-$Rb_2Sb_4S_7$,[7,8] $Cs_6Sb_{10}S_{18}\cdot 1.2H_2O$,[9] $K_2Sb_4S_7\cdot H_2O$,[10] $K_2Sb_4S_7$,[11] and $TlSb_3S_5$.[12] The Sb^{3+} compounds exhibit structural diversity due to the stereochemical effect of the inert lone pair and the tendency of Sb to adopt three-,[13] four-,[14] or five-coordination.[4]

To further explore antimony sulfides from a new synthetic angle, the alkali metal polychalcogenide flux method was used. This method has proven to be an extremely useful low-temperature route to access novel compounds.[15] Since there are no known solid-state antimony sulfides containing polysulfide ligands, we investigated the utility of this synthetic method in obtaining such compounds. We report here the synthesis, properties, and structural characterization of two new compounds, $Cs_2Sb_4S_8$ **(I)** and $CsSbS_6$ **(II)**, which represent the first two examples of solid-state antimony compounds containing polysulfide ligands. $Cs_2Sb_4S_8$ is isostructural with $Cs_2Sb_4Se_8$,[16] while **II** represents a new structure type.

Experimental Section

Reagents. Chemicals in this work were used as obtained: (i) antimony powder, 99.999+% purity, –200 mesh, Cerac Inc., Milwaukee, W; (ii) sulfur powder, sublimed, J. T. Baker Chemical Co., Phillipsburg, NJ; (iii) cesium metal, analytical reagent, Johnson Matthey/AESAR Group, Seabrook, NH; (iv) methanol, anhydrous, Mallinckrodt Inc., Paris, KY; (v) diethyl ether, ACS anhydrous, EM Science, Inc., Gibbstown, NJ.

Syntheses. All manipulations were carried out under a dry nitrogen atmosphere in a Vacuum Atmospheres Dri-Lab glovebox. For the preparation of Cs_2S, we used a modified literature procedure.[17]

Dicesium Octasulfidotetraantimonate(III), $Cs_2Sb_4S_8$ (I). An amount of 0.061 g (0.5 mmol) of Sb, 0.164 g (0.55 mmol) of Cs_2S, and 0.128 g (4.00 mmol) of S were thoroughly mixed and transferred to a 6-mL Pyrex tube which was subsequently flamed-sealed in vacuo ($\sim 10^{-3}$ Torr). The reaction mixture was heated to 280 °C over 12 h in a computer-controlled furnace. It was kept at 280 °C for 5 days, followed by cooling to 100 °C at a rate of 2 °C/h and then to room temperature in 1 h. The product, which is stable in water and air, was isolated by dissolving the Cs_2S_x flux with methanol under inert atmosphere to give orange-red crystals and orange powder. Quantitative microprobe analysis on single crystals gave $CsSb_{1.9}S_{4.2}$ (average of four data acquisitions), while analysis of the orange powder gave $Cs_{2.1}SbS_{3.9}$ (average of three data acquisitions). The orange powder was removed by washing with ethylenediamine,

† A. P. Sloan Foundation Fellow, 1991–3, and Camille and Henry Dreyfus Teacher Scholar, 1993–5.

® Abstract published in *Advance ACS Abstracts,* February 15, 1994.

(1) (a) Olivier-Fourcade, E.; Phillippot, J.; Maurin, M. *Z. Anorg. Allg. Chem.* **1978**, *446*, 159–168. (b) Graf, H. A.; Schafer, H. *Z. Anorg. Allg. Chem.* **1975**, *414*, 211–219. (c) Kanishcheva, A. S.; Kuznetsov, V. G.; Lazarev, V. B.; Tarasova, T. G. *Zh. Strukt. Khim.* **1977**, *18*, 1069. (d) Kanishcheva, A. S.; Mikhailov, Y. N.; Kuznetsov, V. G.; Batog, V. N. *Dokl. Akad. Nauk SSSR* **1980**, *251*, 603–605.
(2) Cordier, G.; Schafer, H. *Rev. Chim. Miner.* **1981**, *18*, 218–223.
(3) Dorrscheidt, W.; Schafer, H. *Z. Naturforsch.* **1981**, *36B*, 410–414.
(4) Cordier, G.; Schwidetzky, C.; Schafer, H. *Rev. Chim. Miner.* **1982**, *19*, 179–186.
(5) Parise, J. B.; Ko, Y. *Chem. Mater.* **1992**, *4*, 1446–1450.
(6) Sheldrick, W. S.; Hausler, H.-J. *Z. Anorg. Allg. Chem.* **1988**, *561*, 149–156.
(7) Dittmar, V. G.; Schafer, H. *Z. Anorg. Allg. Chem.* **1978**, *441*, 93–97.
(8) Sheldrick, W. S.; Hausler, H.-J. *Z. Anorg. Allg. Chem.* **1988**, *557*, 105–111.
(9) Parise, J. B. *J. Chem. Soc., Chem. Commun.* **1990**, *22*, 1553–1554.
(10) Eisenmann, B.; Schafer, H. *Z. Naturforsch.* **1979**, *34B*, 383–385.
(11) Graf, H. A.; Schafer, H. *Z. Naturforsch.* **1972**, *27B*, 735–739.
(12) Gostojic, M.; Nowacki, W.; Engle, P. *Z. Kristallogr.* **1982**, *159*, 217–224.
(13) Dittmar, V. G.; Schafer, H. *Z. Anorg. Allg. Chem.* **1977**, *437*, 183–187.
(14) Cordier, G.; Schafer, H.; Schwidetzky, C. *Z. Anorg. Allg. Chem.* **1984**, *39b*, 131–134.
(15) (a) Kanatzidis, M. G. *Chem. Mater.* **1990**, *2*, 353–363. (b) Kanatzidis, M. G.; Park, Y. *J. Am. Chem. Soc.* **1990**, *111*, 3767–3769. (c) Kanatzidis, M. G.; Park, Y. *Chem. Mater.* **1990**, *2*, 99–101. (d) Park, Y.; Kanatzidis, M. G. *Angew. Chem., Int. Ed. Engl.* **1990**, *29*, 914–915. (e) Sunshine, S. A.; Kang, D.; Ibers, J. A. *J. Am. Chem. Soc.* **1987**, *109*, 6202–6204. (f) Kang, D.; Ibers, J. A. *Inorg. Chem.* **1988**, *27*, 549–551.
(16) Sheldrick, W. S.; Kaub, J. *Z. Anorg. Allg. Chem.* **1986**, *536*, 114–118.
(17) Feher, F. In *Handbuch der Praparativen Anorganischen Chemie;* Brauer, G., Ed.; Ferdinand Enke: Stuttgart, Germany, 1954; pp 280–281.

0020-1669/94/1333-1205$04.50/0

Table 1. Calculated and Observed X-ray Powder Diffraction Patterns for $Cs_2Sb_4S_8$

hkl	d_{calcd}, Å	d_{obsd}, Å	I/I_{max}(obsd), Å
010	9.44	9.60	6
011	5.19	5.24	6
$\bar{1}10$	4.96	5.00	3
020	4.72	4.76	6
101	3.97	4.00	18
111	3.81	3.84	8
021	3.77	3.80	34
$\bar{1}\bar{2}1$	3.70	3.73	17
$\bar{1}20$	3.54	3.56	15
$\bar{2}01$	3.21	3.22	18
030	3.15	3.16	6
$\bar{1}02$	3.10	3.12	26
130	3.03	3.04	3
$1\bar{2}1$	2.89	2.90	100
$0\bar{3}1$	2.79	2.80	7
$\bar{1}30$	2.66	2.67	4
022	2.59	2.60	4
$0\bar{2}2$	2.56	2.57	5
$\bar{2}21$	2.480	2.488	4
$2\bar{1}1$	2.417	2.424	3
140	2.341	2.352	6
122	2.307	2.316	11
$\bar{1}\bar{4}1$	2.248	2.257	7
041	2.213	2.222	4
$\bar{2}22$	2.156	2.157	5
300	2.144	2.145	3
$\bar{1}40$	2.107	2.115	4
$\bar{1}\bar{1}3$	2.083	2.076	3
003	2.051	2.055	3
$3\bar{2}2$	1.958	1.963	9
$\bar{1}23$	1.904	1.909	8
150	1.896	1.894	6
042	1.885	1.882	8
$0\bar{2}3$	1.872	1.867	3
$\bar{3}20$	1.843	1.848	4
$2\bar{2}2$	1.762	1.765	4
$\bar{3}03$	1.717	1.720	3
$4\bar{2}1$	1.656	1.659	2
$\bar{2}42$	1.646	1.650	3
$\bar{4}02$	1.603	1.607	3
160	1.588	1.593	3
$\bar{2}43$	1.581	1.584	3

followed by water, MeOH, and ether to give 0.084 g (67% yield based on Sb) of the pure orange-red rectangular blocklike crystals. Far-IR (CsI matrix) gave six absorbances at 341 (w), 328 (w), 308 (m), 304 (m), 236 (m), and 233 cm^{-1} (m).

Cesium Hexasulfidoantimonate(III), $CsSbS_6$ (II). The reaction of 0.061 g (0.500 mmol) of Sb, 0.149 g (0.500 mmol) of Cs_2S, and 0.144 g (4.5 mmol) of S at 260 °C for 5 days followed by isolation in methanol gave 0.155 g (69% yield based on Sb) of dark orange rectangular platelike crystals (air stable). The crystals are insoluble in water but are soluble in ethylenediamine. Quantitative microprobe analysis on the single crystals gave $Cs_{1.2}Sb_{1.0}S_{6.4}$ (average of three data acquisitions.). Far-IR (CsI matrix) gave nine absorbances at 484 (m), 473 (m), 448 (w), 365 (s), 282 (s), 255 (s), 248 (s), 226 (m), and 195 cm^{-1} (s).

Physical Measurements. FT-IR spectra of I and II were recorded as solids in a CsI matrix. The samples were ground with dry CsI into a fine powder and pressed into translucent pellets. The spectra were recorded in the far-IR region (600–100 cm^{-1}, 4-cm^{-1} resolution) with the use of a Nicolet 740 FT-IR spectrometer equipped with a TGS/PE detector and silicon beam splitter. Raman spectra were recorded with a Nicolet FT-Raman 950 spectrometer. Quantitative microprobe analyses of the compounds were performed with a JEOL JSM-35C scanning electron microscope (SEM) equipped with a Tracor Northern energy dispersive spectroscopy (EDS) detector. Data acquisition was performed with an accelerating voltage of 20 kV and a 1-min accumulation time.

Optical diffuse reflectance measurements were made at room temperature with a Shimadzu UV-3101PC double-beam, double-monochromator spectrophotometer operating in the 200–2500-nm region. The instrument was equipped with an integrating sphere and controlled by a personal computer. The measurement of diffuse reflectivity can be used to obtain values for the band gap which agree rather well with values obtained by absorption measurements on single crystals of the same material. The digitized spectra were processed using the Kaleidagraph software program. $BaSO_4$ powder was used as reference (100% reflectance). Absorption data were calculated from the reflectance data using the Kubelka–Munk function:[18]

$$\alpha/S = (1 - R)^2/2R$$

R is the reflectance at a given wavelength, α is the absorption coefficient, and S is the scattering coefficient. The scattering coefficient has been shown to be practically wavelength independent for particles larger than 5 μm, which is smaller than the particle size of the samples used here.[18a,b]

Differential thermal analysis (DTA) was performed with a computer-controlled Shimadzu DTA-50 thermal analyzer. The ground single crystals (~10.0 mg total mass) were sealed in quartz ampules under vacuum. An empty quartz ampule of equal mass was sealed and placed on the reference side of the detector. The samples were heated to the desired temperature at 10 °C/min and then isothermed for 10 min followed by cooling at 10 °C/min to 100 °C and finally by rapid cooling to room temperature. Cooling rates as low as 3 °C/min gave similar results. The reported DTA temperatures are peak temperatures. The DTA samples were examined by powder X-ray diffraction after the experiments.

Crystallographic Studies. Both compounds were examined by X-ray powder diffraction (XRD) for the purpose of phase purity and identi-

Table 2. Calculated and Observed X-ray Powder Diffraction Patterns for $CsSbS_6$

hkl	d_{calcd}, Å	d_{obsd}, Å	I/I_{max}(obsd)
011	8.67	8.65	6
020	7.21	7.19	17
021	6.00	6.00	5
002	5.43	5.41	8
012	5.08	5.06	13
101	4.71	4.70	3
111	4.48	4.49	4
031	4.39	4.40	3
022	4.33	4.33	2
$\bar{1}12$	4.23	4.22	8
121	3.94	3.93	2
$\bar{1}31$	3.64	3.64	20
032	3.60	3.60	100
112	3.49	3.50	2
041	3.42	3.41	12
131	3.36	3.36	7
023	3.23	3.23	37
140	3.06	3.05	4
$\bar{2}11$	2.88	2.88	7
103	2.82	2.81	3
051	2.79	2.78	18
004	2.71	2.71	10
014	2.67	2.66	9
123	2.62	2.62	7
024	2.54	2.54	5
$\bar{1}24$	2.51	2.50	4
$\bar{1}43$	2.468	2.464	1
060	2.402	2.399	30
$\bar{2}23$	2.375	2.374	3
240	2.250	2.249	2
143	2.219	2.217	3
062	2.196	2.194	5
044	2.167	2.164	12
$\bar{1}44$	2.146	2.142	12
232	2.114	2.111	2
$\bar{2}51$	2.057	2.056	2
063	2.000	2.000	1
$\bar{1}54$	1.959	1.957	2
072	1.925	1.923	15
115	1.891	1.885	1
260	1.845	1.842	1
163	1.828	1.828	2
064	1.798	1.798	5
135	1.773	1.771	2
026	1.754	1.753	2
055	1.734	1.727	27
$\bar{3}14$	1.730	1.733	21
$\bar{1}74$	1.631	1.630	2
244	1.611	1.612	5
$\bar{2}55$	1.605	1.606	3

(18) (a) Wendlandt, W. W.; Hecht, H. G. *Reflectance Spectroscopy*; Interscience Publishers: New York, 1966. (b) Kotüm, G. *Reflectance Spectroscopy*; Springer Verlag: New York, 1969. (c) Tandon, S. P.; Gupta, J. P. *Phys. Status Solidi* **1970**, *38*, 363–367.

Table 3. Summary of Crystallographic Data for $Cs_2Sb_4S_8$ and $CsSbS_6$

	I	II
formula	$Cs_2Sb_4S_8$	$CsSbS_6$
fw	504.65	447.02
a, Å	6.743(1)	5.885(2)
b, Å	9.577(2)	14.413(2)
c, Å	6.367(1)	11.079(2)
α, deg	91.63(1)	90.000
β, deg	104.83(1)	101.69(2)
γ, deg	80.57(1)	90.000
Z; V, Å^3	1; 392	4; 920
λ, Å	0.710 73	0.710 73
space group	$P\bar{1}$ (No. 2)	$P2_1/n$ (No. 14)
d_{calc}, g/cm^3	4.275	3.226
μ(Mo Kα), cm^{-1}	124.08	81.158
T, °C	23	23
final R/R_w,[a] %	3.2/4.9	2.5/3.9

[a] $R = \sum(|F_o| - |F_c|)/\sum|F_o|$; $R_w = [\sum w(|F_o| - |F_c|)^2/\sum w|F_o|^2]^{1/2}$.

Table 4. Fractional Atomic Coordinates and B_{eq} Values for $Cs_2Sb_4S_8$ with Estimated Standard Deviations in Parentheses

atom	x	y	z	B_{eq},[a] Å^2
Cs(1)	0.16496(7)	0.06678(5)	1.32325(8)	1.83(2)
Sb(1)	−0.18018(7)	0.45220(5)	0.66230(8)	1.51(2)
Sb(2)	0.40888(7)	0.32190(5)	0.92176(8)	1.42(2)
S(1)	−0.1566(3)	0.4058(2)	0.2934(3)	1.53(7)
S(2)	0.5781(3)	0.0751(2)	1.0945(3)	1.65(7)
S(3)	0.0745(3)	0.2366(2)	0.8152(3)	1.49(6)
S(4)	0.5233(3)	0.2837(2)	0.5893(3)	1.73(7)

[a] B values for anisotropically refined atoms are given in the form of the isotropic equivalent displacement parameter defined as $B_{eq} = (4/3)[a^2B(1,1) + b^2B(2,2) + c^2B(3,3) + ab(\cos\gamma)B(1,2) + ac(\cos\beta)B(1,3) + bc(\cos\alpha)B(2,3)$.

Table 5. Fractional Atomic Coordinates and B_{eq} Values for $CsSbS_6$ with Estimated Standard Deviations in Parentheses

atom	x	y	z	B_{eq},[a] Å^2
Cs	−0.0826(1)	0.40998(4)	0.18541(5)	2.82(2)
Sb	0.02834(8)	0.09589(4)	0.11379(4)	1.62(2)
S(1)	−0.0049(4)	0.0694(1)	−0.1242(2)	2.05(7)
S(2)	0.1085(4)	0.0673(2)	0.3633(2)	2.37(7)
S(3)	0.0089(3)	0.1923(2)	0.4244(2)	2.28(7)
S(4)	−0.3439(4)	0.1818(2)	0.4124(2)	2.37(8)
S(5)	0.5085(3)	0.2270(1)	0.2373(2)	2.10(7)
S(6)	0.4558(3)	0.1142(1)	0.1209(2)	1.90(7)

[a] B values for anisotropically refined atoms are given in the form of the isotropic equivalent displacement parameter defined as $B_{eq} = (4/3)[a^2B(1,1) + b^2B(2,2) + c^2B(3,3) + ab(\cos\gamma)B(1,2) + ac(\cos\beta)B(1,3) + bc(\cos\alpha)B(2,3)$.

fication. Accurate d_{hkl} spacings (angstroms) were obtained from the powder patterns recorded on a Rigaku rotating-anode (Cu Kα) X-ray powder diffractometer, Rigaku-Denki/RW400F2 (Rotaflex), at 45 kV and 100 mA with a 1°/min scan rate. The results are summarized in Tables 1 and 2.

Single-crystal X-ray diffraction data were collected on a Rigaku AFC6 diffractometer, and the $\omega/2\theta$ scan technique was used. Graphite-monochomatized radiation was used. Neither crystal showed any significant intensity decay, as judged by three check reflections measured every 150 reflections throughout the data collection. The space groups were determined from systematic absences and intensity statistics. The structures were solved by direct methods of SHELXS-86[19] and refined by full-matrix least-squares techniques of the TEXSAN package of crystallographic programs.[20] The secondary extinction coefficient was refined for both structures. An empirical absorption correction based on ψ scans was applied to each data set, followed by a DIFABS[21] correction to the isotropically refined structure. The atomic scattering factors were obtained from ref 20. All atoms were eventually refined anisotropically. All calculations were performed on a VAXstation 3100/76 computer.

(19) Sheldrick, G. M. In *Crystallographic Computing 3*; Sheldrick, G. M., Kruger, C., Doddard, R., Eds.; Oxford University Press: Oxford, England, 1985; pp 175–189.
(20) *TEXSAN: Single Crystal Structure Analysis Software*, Version 5.0; Molecular Structure Corp.: The Woodlands, TX 77381, 1981.
(21) Walker, N.; Stuart, D. *Acta Crystallogr.* **1983**, *A39*, 158–166.

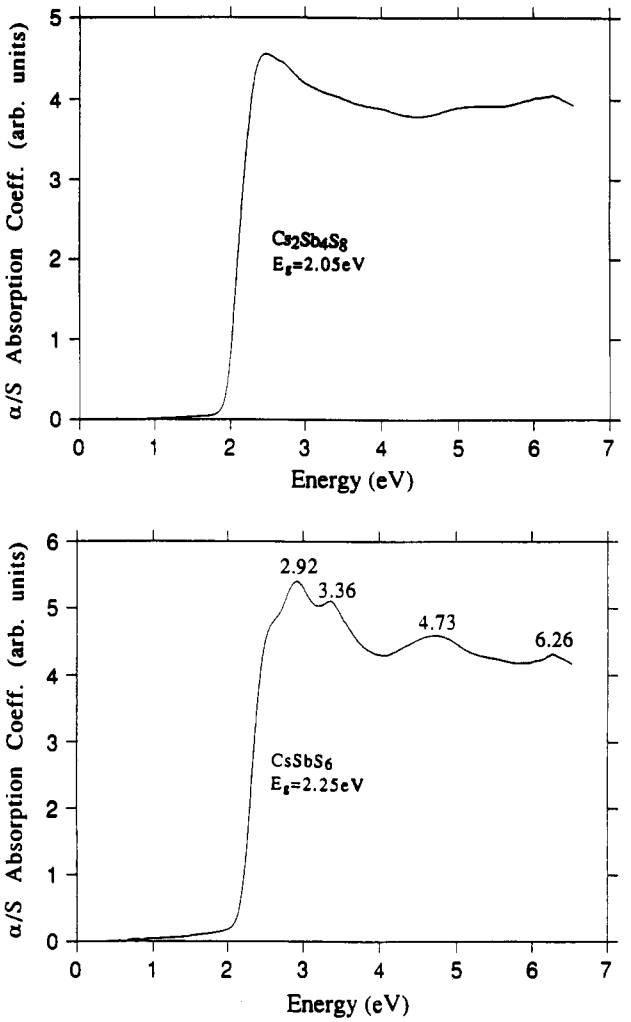

Figure 1. (A) Top: Optical absorption spectrum of $Cs_2Sb_4S_8$. (B) Bottom: Optical absorption spectrum of $CsSbS_6$.

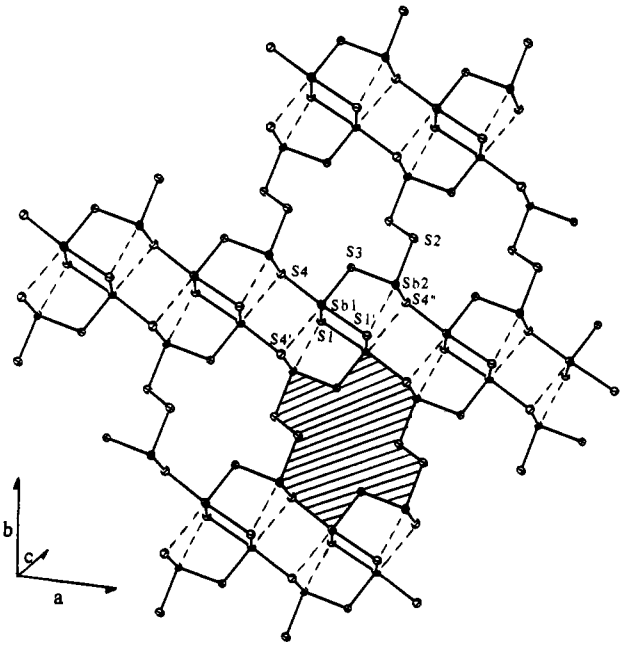

Figure 2. Two-dimensional structure of the $[Sb_4S_8]_n^{n-}$ anionic framework with labeling as drawn by ORTEP. The dashed lines represent Sb–S long interactions in the range 3.022(2)–3.277(2) Å. The shaded area outlines the 14-membered Sb/S rings in the structure.

During the structural refinement of $CsSbS_6$, an $R/R_w = 3.0/5.1$ was obtained. After the final least squares cycle, the (10&$\bar{1}$) and (002) reflections were observed to have abnormally high $\Delta F/\sigma(F)$ values at

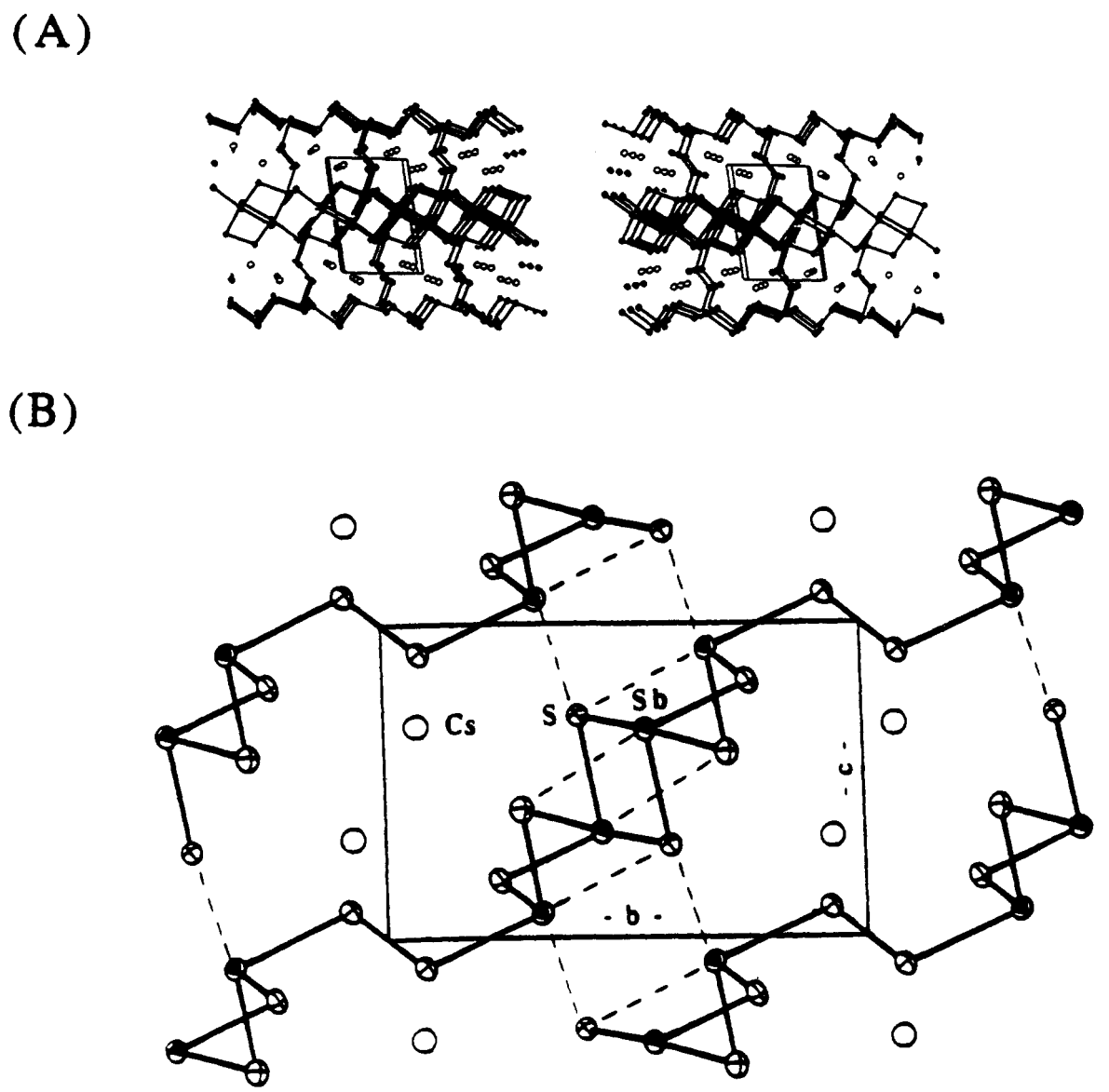

Figure 3. (A) Stereoview of $Cs_2Sb_4S_8$ viewed down the [001] direction. (B) Packing diagram of $Cs_2Sb_4S_8$ showing a projection in the [100] direction. The dashed lines represent long Sb–S interactions underscoring the pseudo-3D character of the structure. The shaded ellipsoids are Sb atoms, and the open ellipsoids are Cs atoms.

−118.73 and 72.52, respectively. Since we suspected that these two low 2θ reflections might not have been measured properly due to close proximity to the beam stop, we eliminated them from the calculation. Least-squares refinement gave R/R_w = 2.9/4.0 while the Sb–S bond length standard deviations improved from 0.003 to 0.002.

The complete data collection parameters and details of the structure solution and refinement for both compounds are given in Table 3. The coordinates of all atoms, average temperature factors, and their estimated standard deviations for both compounds are given in Tables 4 and 5.

Results and Discussion

Synthesis and Spectroscopy. The syntheses of $Cs_2Sb_4S_8$ and $CsSbS_6$ were a result of a redox reaction in which the Sb metal is oxidized by polysulfide ions to give Sb^{3+} species. $CsSbS_6$ was formed from a $Sb/Cs_2S/S$ ratio of 1/1/9 at 260 °C while $Cs_2Sb_4S_8$ could be obtained at 280 °C with a ratio of 1/(0.9–1.1)/8. $Cs_2Sb_4S_8$ appears to be more thermodynamically stable than $CsSbS_6$ under the same acidic flux conditions. This is supported by thermal analysis data which reveal that $CsSbS_6$ decomposes to $Cs_2Sb_4S_8$ upon heating (vide infra).

The IR spectroscopic data for $CsSbS_6$ show absorptions at 484, 473, and 448 cm^{-1}, which we assign to S–S stretching vibrations. Similar absorbances were not observed for $Cs_2Sb_4S_8$ because the S–S bond resides on a center of symmetry. However, the S–S stretching mode is Raman-active and occurs at 474 cm^{-1}. The absorbances found at lower energy for $CsSbS_6$ (365–195 cm^{-1}) and $Cs_2Sb_4S_8$ (341–233 cm^{-1}) have been tentatively assigned as Sb–S vibrations.

The optical properties of **I** and **II** were assessed by studying the UV/near-IR reflectance spectra of the materials. The spectra confirm the semiconductor nature of the materials by revealing the presence of sharp optical gaps as shown in Figure 1. Both compounds exhibit steep absorption edges from which the band gap, E_g, can be assessed at 2.05 and 2.25 eV, respectively. By comparison, the corresponding band gap of Sb_2S_3 is 1.7 eV.[22] A linear relationship is found for both compounds if the square of the absorption coefficient, $(\alpha/S)^2$, is plotted vs $(E-E_g)$, suggesting that the band gaps are direct in nature.[23] However, independent confirmation is needed to verify this conclusion. The relatively good air and moisture stability of $Cs_2Sb_4S_8$ and its excellent optical transparency below 2.05 eV make it a good candidate for exploration of its linear and nonlinear optical properties. The optical absorption spectrum of **II** also features absorbances at higher energy which are due to other electronic transitions in the solid, perhaps within the S_5^{2-} fragment.

(22) Bube, R. H. *Photoconductivity of Solids*; John Wiley and Sons, Inc.: New York, 1960; pp 233–235.
(23) Pankove, J. I. *Optical Processes in Semiconductors*; Dover Publications: New York, 1975.

Table 6. Selected Distances (Å) and Angles (deg) in $Cs_2Sb_4S_8$ with Standard Deviations in Parentheses[a]

Sb(1)–S(1)	2.418(2)	S(1′)–Sb(1)–S(3)	87.79(6)
Sb(1)–S(1′)	2.783(2)	S(1′)–Sb(1)–S(4)	171.50(6)
Sb(1)–S(3)	2.501(2)	S(3)–Sb(1)–S(4′)	173.65(6)
Sb(1)–S(4)	2.712(2)	S(1)–Sb(1)–S(1′)	86.47(6)
Sb(1)–S(4′)	3.277(2)	S(1)–Sb(1)–S(3)	93.85(7)
Sb(2)–S(1′)	3.022(2)	S(1′)–Sb(2)–S(1″)	107.81(4)
Sb(2)–S(1″)	3.456(2)	S(1′)–Sb(2)–S(2)	172.22(5)
Sb(2)–S(2)	2.592(2)	S(1′)–Sb(2)–S(3)	83.55(6)
Sb(2)–S(3)	2.449(2)	S(1′)–Sb(2)–S(4″)	85.67(6)
Sb(2)–S(4″)	2.430(2)	S(1″)–Sb(2)–S(2)	79.18(5)
		S(1″)–Sb(2)–S(3)	154.03(6)
S(2)–S(2′)	2.092(4)		
Sb(1)–Sb(1′)	3.798(1)	S(1″)–Sb(2)–S(4″)	103.23(6)
Sb(1)–Sb(2)	3.898(1)	S(2)–Sb(2)–S(4″)	96.18(7)
Sb(2)–Sb(2′)	3.833(1)	S(3)–Sb(2)–S(4″)	100.83(7)
Cs–Cs′	3.913(1)		
Cs–S(1)	3.576(2)	Cs–S(3)	3.527(2)
Cs–S(2)	3.470(2)	Cs–S(3′)	3.632(2)
Cs–S(2′)	3.839(2)	Cs–S(3″)	3.534(2)
Cs–S(2″)	3.648(2)	Cs–S(4″)	3.518(2)
Cs–S(2‴)	3.850(2)	Cs–S(4‴)	3.632(2)
av Cs–S	3.62(4)		

[a] The estimated standard deviations in the mean bond lengths and the mean bond angles are calculated by the equations $\sigma_l = [\sum_n (l_n - l)^2/n(n-1)]^{1/2}$, where l_n is the length (or angle) of the nth bond, l the mean length (or angle), and n the number of bonds.

Description of Structures. Structure of $Cs_2Sb_4S_8$ (I). Compound I is isostructural with the hydrothermally prepared $Cs_2Sb_4Se_8$.[16] At the most fundamental level, this structure is made up of condensed SbS_3^{3-} pyramids and S_2^{2-} units. Although, overall this structure is three-dimensional, it is assembled by cross-linking one-dimensional $[Sb_4S_6]$ parallel chains with disulfide ligands to form sheets that are parallel to the (011) crystallographic plane. Figure 2 shows a view of an individual layer of $[Sb_4S_8]_n^{n-}$. The layer can alternatively be described as being composed of 14-membered rings of alternating Sb–S atoms and S_2 units. The rings are connected in two dimensions by Sb–S–Sb linkages to form the layer. The layers stack one on top of the other with their 14-membered rings in registry so that they form channels running down the c axis. The channels are clearly visible in Figure 3A. Long Sb–S interactions (3.456(2) Å) between sheets give rise to a second set of channels running down the a axis that are filled with 10-coordinate Cs^+ ions (Cs–S mean = 3.62(4) Å) (Figure 3B). Due to these long Sb–S interactions between the sheets, the structure possesses pseudo-three-dimensional character. Selected bond distances and bond angles for I are given in Table 6.

Sb(1) is found in a distorted square pyramidal coordination due to the stereochemically active lone pair at the base of the pyramid. This type of coordination is found in Sb_2S_3 (stibnite).[24] The four Sb(1)–S bonds range from 2.418(2) to 2.783(2) Å with a fifth coordination site occupied by a weakly interacting S(4) that has a distance of 3.277(2) Å (Figure 2). This distance is considerably shorter than the sum of the Sb–S van der Waals radii (4.05 Å).[25] These distances, ranging from the Sb–S bond at 2.418(2) Å to the weaker interaction at 3.277(2) Å, are very comparable to those found in other ternary antimony(III) sulfides, such as $Cs_3Sb_5S_9$[5] and β-$Rb_2Sb_4S_7$.[8]

The coordination environment of Sb(2) could be described as a trigonal pyramid with three bonds ranging from 2.440(2) to 2.592(2) Å (Figure 2). Sb(2) is also interacting with two sulfur atoms along the top of the trigonal pyramid. A strong interaction is found at 3.022(2) Å with S(1), and a weak interaction is observed with S(1″) at 3.456(2) Å. This type of coordination is observed in Sb_2S_3 (Sb 1)[24] and $CsSbS_2$.[1d]

Structure of $CsSbS_6$ (II). $CsSbS_6$ is the first example of a solid-state antimony polysulfide compound. The only other known antimony polysulfide is the molecular dimeric antimony polysulfide complex $[Sb_2S_{15}]^{2-}$ that was recently prepared by Rauchfuss et al.[26] The novel one-dimensional structure of II is composed of Sb_2S_2 rhombi that are linked along the a axis by pentasulfide ligands to form chains (Figure 4A). The formula can alternatively be expressed as $CsSbS(S_5)$. These chains are separated by nine-coordinate Cs^+ ions (mean Cs–S distance = 3.69(3) Å). Figure 4B shows the packing diagram of $CsSbS_6$, along the a axis (chain axis). Selected bond distances and bond angles for I are given in Table 7.

Sb is bonded to four sulfur atoms with bond distances ranging from 2.390(2) to 2.737(2) Å. The coordination around the Sb

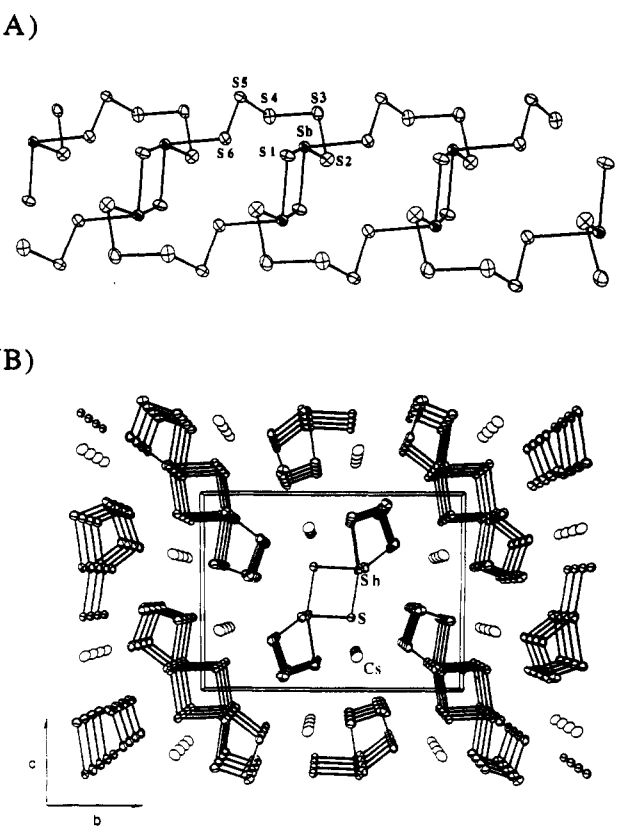

Figure 4. (A) Structure of a single $(SbS_6)_n^{n-}$ chain with labeling. (B) Packing diagram of $CsSbS_6$ viewed down the a axis (chain axis). The shaded ellipsoids are Sb atoms, and the open ellipsoids are Cs atoms.

Table 7. Selected Distances (Å) and Angles (deg) for $CsSbS_6$ with Standard Deviations in Parentheses[a]

Sb–S(6)	2.515(2)	S(2)–S(3)	2.052(3)
Sb–S(2)	2.737(2)	S(3)–S(4)	2.060(3)
Sb–S(1)	2.635(2)	S(4)–S(5)	2.063(3)
Sb–S(1′)	2.390(2)	S(5)–S(6)	2.057(2)
av Sb–S	2.57(8)	av S–S	2.058(2)
		Sb–Sb′	3.711(2)
Cs–S(1)	3.582(2)	Cs–S(5)	3.693(2)
Cs–S(6)	3.629(2)	Cs–S(2)	3.718(2)
Cs–S(1′)	3.630(2)	Cs–S(2′)	3.786(2)
Cs–S(3)	3.676(2)	Cs–S(4)	3.822(2)
Cs–S(2)	3.679(2)	av Cs–S	3.69(3)
S(6)–Sb–S(2)	90.87(6)	Sb–S(6)–S(5)	97.23(8)
S(6)–Sb–S(1)	85.31(6)	Sb–S(2)–S(3)	101.41(9)
S(6)–Sb–S(1′)	99.81(6)	S(2)–S(3)–S(4)	105.4(1)
S(2)–Sb–S(1)	162.10(6)	Sb–S(1)–Sb	95.08(6)
S(2)–Sb–S(1′)	78.47(6)	S(6)–S(5)–S(4)	108.7(1)
S(1)–Sb–S(1′)	84.91(6)	S(3)–S(4)–S(5)	105.3(1)

[a] The estimated standard deviations in the mean bond lengths and the mean bond angles are calculated by the equations $\sigma_l = [\sum_n (l_n - l)^2/n(n-1)]^{1/2}$, where l_n is the length (or angle) of the nth bond, l the mean length (or angle), and n the number of bonds.

(24) Hofmann, W. *Z. Kristallogr.* **1933**, *86*, 225.
(25) Pauling, L. *The Nature of the Chemical Bond*, 3rd ed.; Cornell University Press: Ithaca, NY, 1966; p 260.
(26) Partha, P. P.; Rauchfuss, T. B.; Wilson, S. R. Preprint.

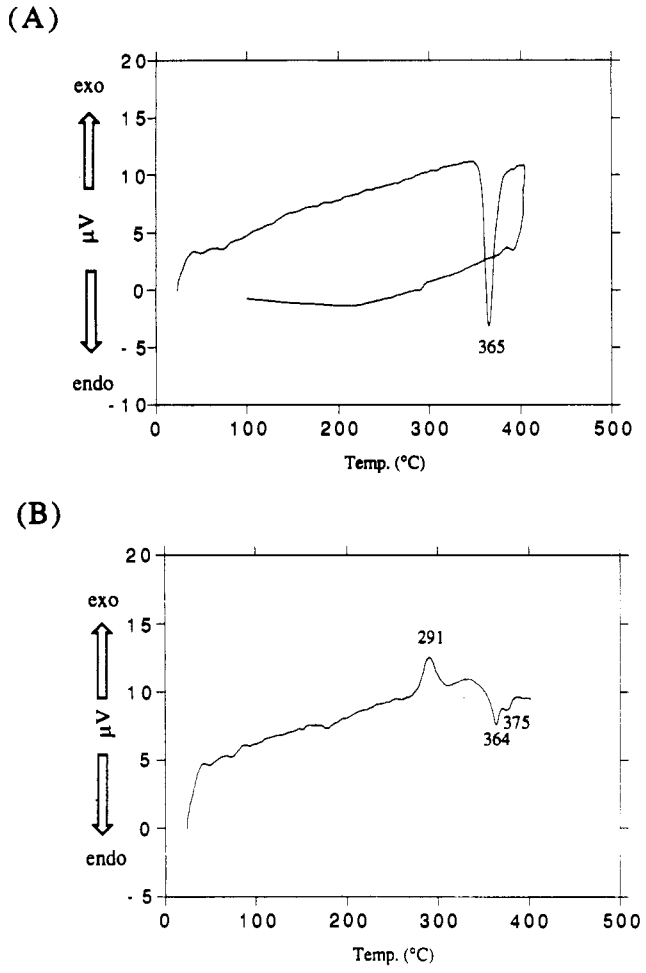

Figure 5. (A) Differential thermal analysis (DTA) data for $Cs_2Sb_4S_8$ showing the first heating and cooling cycle. Heat is absorbed at 365 °C as the material melts but is not released upon cooling. (B) Data for reheating showing the crystallization of $Cs_2Sb_4S_7$ at 291 °C, followed by melting of the excess glass at 364 and 375 °C.

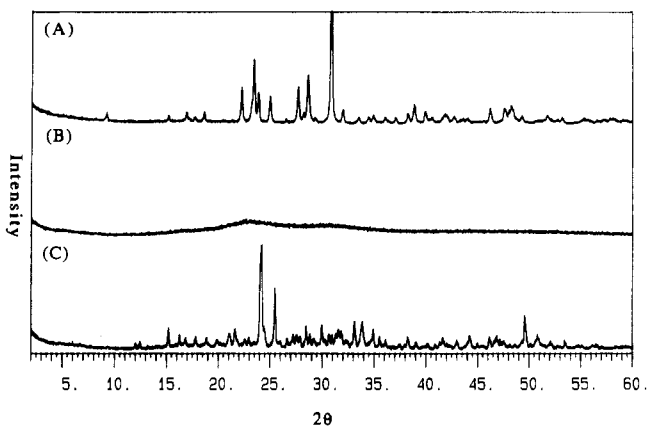

Figure 6. X-ray diffraction patterns: (A) $Cs_2Sb_4S_8$ single crystals; (B) material heated to 400 °C and then cooled (glassy state); (C) material after reheating to 310 °C (crystallization of $Cs_2Sb_4S_7$).

atom (including the lone pair) is trigonal bipyramidal with the lone pair at the equatorial position. The repulsion by the lone pair gives rise to a nearly axial S(2)–Sb–S(1) angle of 162.10(6)° and an S(1′)–Sb–S(6) angle of 99.81(6)° in the trigonal plane. The two axial Sb–S bonds (2.635(2), 2.737(2) Å) are longer than the two equatorial bonds (2.390(2), 2.515(2) Å). This combination of Sb coordination and variation in bond length has been seen for Sb(3) of $Cs_2Sb_4S_7$,[27] where the axial bond lengths of 2.637(4) and 2.739(5) Å and equatorial bond lengths of 2.456(5) and 2.500(5) Å were observed. Several other phases have demonstrated these characteristics including β-$Rb_2Sb_4S_7$ (Sb 1,2),[8] $RbSbS_2$ (Sb 1,2),[1c] $SrSb_4S_7{\cdot}6H_2O$ (Sb 4),[12] and $Cs_2Sb_8S_{13}$ (Sb 4).[28]

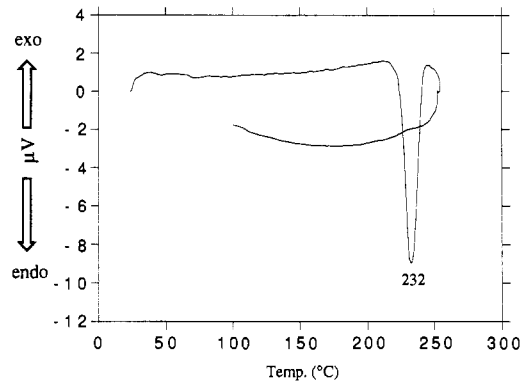

Figure 7. DTA of $CsSbS_6$ showing the endothermic peak at 232 °C corresponding to the decomposition of $CsSbS_6$ to $Cs_2Sb_4S_8$.

Normal S–S bond distances are observed in the μ_2-S_5^{2-} ligand (2.058(5) Å mean). The bridging mode of this ligand has been observed in the one-dimensional solid-state compound $KAuS_5$[29] and the basketlike dimer $[Mo_2(NO)_2(S_2)_3(S_5)(OH)]^{3-}$.[30]

Solid-state compounds containing Q_x^{2-} (Q = S, Se) ligands with $x > 3$ are relatively rare. Some examples include NH_4CuS_4,[31] α,β-$KCuS_4$,[32] $CsCuS_6$,[33] $(NH_4)_2PdS_{11}$,[34] K_2PdSe_{10},[35] $(Ph_4P)AgSe_4$,[36] $(Me_4N)AgSe_5$,[36] $KAuSe_5$,[37] K_3AuSe_{13},[37] and $K_2Sn_2S_8$.[38]

Thermal Analysis. The thermal behavior of **I** and **II** was investigated with differential thermal analysis (DTA). Figure 5A shows that upon heating of $Cs_2Sb_4S_8$, a sharp melting endotherm occurs at 365 °C. Upon cooling, no corresponding exothermic peak is observed, indicating that no crystallization takes place. Red glassy material was observed in the quartz ampule. Powder X-ray diffraction (XRD) of the sample at room temperature gave an amorphous pattern, which confirms the glassy character. Upon subsequent reheating, a broad exotherm at 291 °C was observed, followed by two endothermic peaks at 364 and 375 °C (see Figure 5B). The endotherm at 364 °C may be due to some $Cs_2Sb_4S_8$, but the peak is not always there when runs from different batches are considered. We speculate that occasionally $Cs_2Sb_4S_8$ does not fully convert to glass due to small but significant differences in thermal conditions from run to run. XRD studies show that the exotherm at 291 °C is the result of crystallization of $Cs_2Sb_4S_7$[28,39] from the glassy matrix (see Figure 6). Thus, upon heating, $Cs_2Sb_4S_8$ transforms to $Cs_2Sb_4S_7$ via an intermediate glassy state. The small endotherms at 364 and 375 °C are probably due to melting of excess glassy material and perhaps $Cs_2Sb_4S_7$.

Figure 7 shows that upon heating of $CsSbS_6$, a sharp endotherm occurs at 232 °C. Upon cooling, no exothermic peak is observed,

(27) Dittmar, V. G.; Schafer, H. *Z. Anorg. Allg. Chem.* **1978**, *441*, 98–102.
(28) Volk, K.; Schafer, H. *Z. Naturforsch.* **1979**, *34B*, 1637–1640.
(29) Park, Y.; Kanatzidis, M. G. To be submitted for publication.
(30) Muller, A.; Eltzner, W.; Bogge, H.; Krickemeyer, E. *Angew. Chem., Int. Ed. Engl.* **1983**, *22*, 884–885.
(31) Burschka, C. *Z. Naturforsch.* **1980**, *35B*, 1511–1513.
(32) Kanatzidis, M. G.; Park Y. *J. Am. Chem. Soc.* **1989**, *111*, 3767–3769.
(33) McCarthy, T. J.; Zhang, X.; Kanatzidis, M. G. *Inorg. Chem.* **1993**, *32*, 2944–2948.
(34) Haradem, P. S.; Cronin, J. L.; Krause, R. A.; Katz, L. *Inorg. Chim. Acta* **1977**, *25*, 173–179.
(35) Kim, K.-W.; Kanatzidis, M. G. *J. Am. Chem. Soc.* **1992**, *114*, 4878–4883.
(36) Huang, S.-P.; Kanatzidis, M. G. *Inorg. Chem.* **1991**, *30*, 1455–1466.
(37) Park, Y.; Kanatzidis, M. G. *Angew. Chem., Int. Ed. Engl.* **1990**, *29*, 914–915.
(38) Liao, J.-H.; Varotsis, C.; Kanatzidis, M. G. *Inorg. Chem.* **1993**, *32*, 2453–2462.
(39) Identified as $Cs_2Sb_4S_7$ by X-ray powder diffraction: *Powder Diffraction File—Inorganic Phases*; 1987; Vol. 32, p 214. Five additional low-intensity peaks were also observed which could be due to the presence of a small amount of impurity.

indicating the absence of crystallization. XRD of the sample at room temperature gave $Cs_2Sb_4S_8$ and Cs_2S. The expelled sulfur was observed to deposit on the end of the ampule opposite from the sample. The endothermic peak is due to the decomposition of $CsSbS_6$ to $Cs_2Sb_4S_8$.

In summary, we have synthesized the first two examples of polysulfide ligands in solid-state antimony compounds using Cs_2S_x fluxes at low temperature (<300 °C). **II** decomposes to **I** at 232 °C which, via a glassy state, transforms to $Cs_2Sb_4S_7$ upon reheating. It is remarkable that two new phases could be uncovered in a somewhat crowded antimony/sulfide field. Since it appears that ternary antimony(III) sulfides can form many different structure types, we are expanding our effort in the search for new ternary antimony(III) chalcogenides while focusing on relatively low reaction temperatures. The participation of polychalcogenide ligands in solid-state frameworks promises to yield new solids with relative open or flexible structures. This work provides concrete evidence that intermediate temperatures in combination with alkali metal polychalcogenide fluxes are important reaction media for exploration of new compounds.

Acknowledgment. Financial support from the National Science Foundation (Grant DMR-9202428) is gratefully acknowledged. The X-ray instrumentation used in this work was purchased in part with funds from the National Science Foundation (Grant CHE-8908088). This work made use of the SEM facilities of the Center for Electron Optics at Michigan State University. We thank Professor T. B. Rauchfuss for making ref 26 available to us. We thank Professor C. R. Kannewurf for useful discussions. We also thank Chris Petty of Nicolet Instrument Corp. for recording the Raman spectrum of $Cs_2Sb_4S_8$.

Supplementary Material Available: Tables giving crystal data, atomic coordinates, bond lengths, bond angles, and isotropic and anisotropic thermal parameters (26 pages). Ordering information is given on any current masthead page.